DNA strand separation studied by single molecule force measurements

U. Bockelmann, B. Essevaz-Roulet, and F. Heslot
Laboratoire de Physique de la Matière Condensée, Ecole Normale Supérieure, 24 rue Lhomond, 75005 Paris, France
(Received 26 November 1997)

We have separately attached the two complementary strands of one end of a DNA double helix to a glass slide and a glass microneedle. Displacing the slide away from the needle, the molecule is progressively pulled open and the changing deflection of the needle gives the corresponding variation in the opening force. Force signals which are very rich in detail are reproducibly obtained. The average level and amplitude of the force signal is almost independent of the opening velocity in the interval 20 nm/s to 800 nm/s. A theoretical description based on the assumption of thermal equilibrium allows us to link the measured force curves to the genomic sequence of the DNA. A molecular stick-slip motion is revealed, which in contrast to the dynamics of macroscopic solid friction is a deterministic and reproducible process. This process is considered experimentally and theoretically. [S1063-651X(98)13208-7]

PACS number(s): 87.45.−k, 83.10.−y, 87.80.+s, 87.15.−v

I. INTRODUCTION

Throughout the last years, the field of force measurements on biomolecules has become increasingly active. Atomic force microscopes (AFM) [1,2], optical tweezers [3–5], and glass microneedles [6,7] have been employed to study the intermolecular and intramolecular interaction forces, which for biological systems span a typical range from 10^{-14} to 10^{-9} N. For example, force versus extension relations of single stranded (SS) DNA [8], double stranded (DS) DNA [7,9,10], and the muscle protein titin [11–13] have been experimentally determined. Forces corresponding to the rupture of ligand receptor complexes [14,15] and short DS-oligonucleotide sequences [16,17] have been investigated by AFM. We have recently measured the forces opposing mechanical unzippering of a long DS-DNA molecule [18,19]. This article contains a comprehensive discussion of the physics governing such a process of DNA strand separation by a mechanical constraint. In Sec. II we present the experimental configuration, experimental results on the dependence of the force curves on the opening velocity, and a statistical analysis of the data in terms of correlation functions. Section III is devoted to the theoretical description of the measurements. The process of molecular stick slip is considered in detail in Sec. IV. Section V contains a discussion of our results in relation to published work.

II. EXPERIMENTS

In the first part of this section, we briefly explain the sample preparation steps and the force measurement technique. A more detailed description can be found in [19].

Figure 1 illustrates the experimental configuration. The two strands on one end of a DS-DNA molecule (phage λ, contour length 16.2 μm, known sequence of 48 502 base pairs) are separately attached to a glass slide (via a second λ DS-DNA serving as linker arm) and a bead. Single strand segments of complementary (but not identical) 12 base sequences are present at the opposite ends of a linearized molecule of phage λ DNA. This allows us to selectively address each of the four single strand ends of the double helix by covalently binding different oligonucleotides (short synthetic SS-DNA molecules). The preparation of the molecular construction is done sequentially using commercial oligonucleotides and λ-phage DNA. Employing well known techniques of molecular biology (annealing of complementary sequences followed by ligation that gives a covalent linkage), we attach a digoxigenin (dig) functionalized oligonucleotide to the linker arm DNA (A) and a biotin-functionalized oligonucleotide to the DNA to be opened (B). A molar excess of 10:1 is used in order to displace the chemical reaction from multimer formation to the formation of the DNA-oligonucleotide construction. Subsequently the two DNA molecules are linked using a third oligonucleotide containing a sequence complementary to the second end of the linker arm DNA and a sequence complementary to the biotin-functionalized oligonucleotide (C). The solution containing the molecular construction is purified with a commercial spin column (Amicon 100, separation and removal of the low molecular weight oligonucleotides from the high molecular weight λ DNA) and deposited on a glass microscope slide. The glass slide has been coated with antibodies against digoxigenin (antidig) and specifically anchors the molecular construction through dig-antidig bonding (A). Afterwards streptavidin coated paramagnetic polysterene beads (Dyna, diameter 2.9 μm) are introduced and react with the biotinylated end of the molecular construction. This sample is placed on an inverted microscope. Acting with a weak mag-

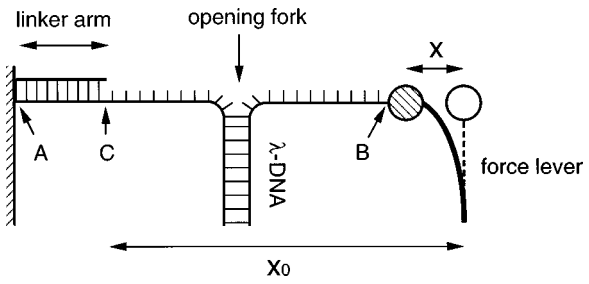

FIG. 1. Schematic view of the molecular construction and the experimental configuration used to unzip a DNA double helix by a mechanical constraint.

netic field, each correctly attached bead moves around a single anchoring point with a tethering length of about 16 μm given by the linker arm DNA. The tip of a biotin functionalized glass microneedle is attached by simply touching such a bead.

The experiments are performed in a solution with nearly physiological salt concentrations (phosphate buffer saline PBS at *p*H7, 10 mM phosphate, 150 mM NaCl). Keeping the base of the lever fixed, the DNA helix is forced open by a lateral displacement x_0 of the microscope slide with a piezo translation stage. A change in the lever deflection x below 0.1 μm can be resolved which corresponds to a force resolution better than 0.2 pN. This is achieved off line, by analyzing a video tape of the microscope image recorded during the opening experiment. A video line crossing the bead is sampled with a constant rate of five or 12 times per second. Each line is converted to a computer file consisting of 640 pixels with 256 gray levels. The resulting numerical spatiotemporal image is low-pass filtered and the bead position is extracted by a thresholding procedure on the black/white contrast of the bead. The filter reduces shot noise caused by mechanical vibrations but does not affect the force signal occurring at lower frequency.

All the data presented in this paper are obtained with a single glass microneedle. This force lever has been prepared with a commercial pipette puller and has about the following dimensions: tip diameter 1 μm, shank diameter 1 mm, tapered length 1 cm. The stiffness of the lever is calibrated with the described setup of the force measurements, but without DNA in the solution. A paramagnetic bead is attached to the lever, then a strong magnet is approached and the lever deflection is measured. Afterwards the bead is detached from the lever with a second microneedle and its acceleration towards the magnet is measured under stroboscopic illumination. Relating the two measurements by the Stokes law of viscous friction we obtain the lever stiffness of $k_{\mathrm{lev}}=1.7\ \ (\pm 0.2) pN/\mu\mathrm{m}$.

It is possible to perform several cycles of opening and closing on the same molecule, by repeatedly increasing and decreasing the sample displacement x_0. During closing sometimes important drops occur in the measured force which we tentatively attribute to a transient delay of the recombination of the single strands. These drops become less frequent and less important in amplitude at smaller displacement velocities. The force signals collected upon opening the molecular construction are reproducible to a high degree of detail, as we will discuss later in this section.

In Fig. 2 a series of force versus displacement curves, corresponding to repeatedly opening the same molecule with different translation velocity, is shown. During the process of DNA strand separation a characteristic force variation between 10 and 15 pN is observed. The gross features of this variation reflect the content of the stronger *G-C* pairs in comparison to the weaker *A-T* pairs, while at a finer scale the signal is influenced by the process of molecular stick slip, as discussed in Sec. IV. The bottom curve of Fig. 2 is a calculation based on the hypothesis of thermal equilibrium, as described in Sec. III. It may therefore be considered as a theoretical result corresponding to the limit of zero displacement velocity. With increasing displacement velocity, the number of details in the measured force curves decreases. At

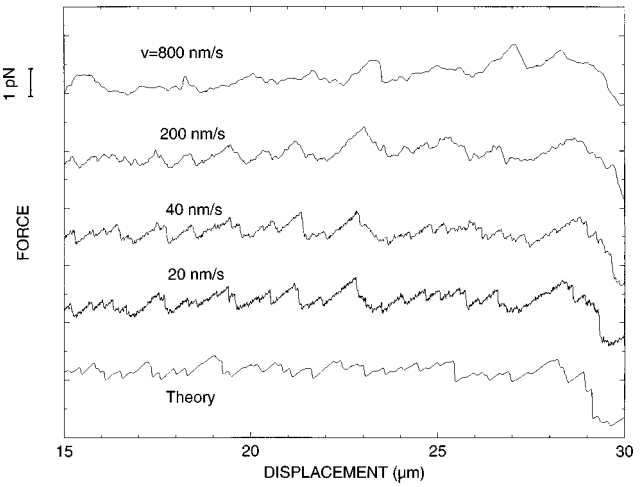

FIG. 2. Force curves measured upon opening a single λ-phage DNA molecule several times with displacement velocities ranging from 20 nm/s to 800 nm/s. A calibrated force lever of stiffness $k_{\mathrm{lev}}=1.7$ pN/μm is used. At the bottom, a force versus displacement curve is shown, which has been calculated according to the description given in Sec. III. The different curves are shifted vertically for clarity. The amplitude of the variations in the force are given by the vertical bar.

800 nm/s, there is a small additional deflection which is probably caused by hydrodynamic drag of the lever.

For quantitative comparison of different force curves, we define a correlation function $g(\Delta)$ by

$$g(\Delta)=\frac{\langle f_1(x')f_2(x'+\Delta)\rangle_{x'}}{\langle f_1(x')^2\rangle_{x'}^{1/2}\langle f_2(x'+\Delta)^2\rangle_{x'}^{1/2}}, \tag{1}$$

where $\langle\ \rangle_{x'}$ stands for an integration over a finite interval (a,b) of displacement; i.e.,

$$\langle f_1(x')f_2(x'+\Delta)\rangle_{x'}=\int_a^b dx' f_1(x')f_2(x'+\Delta). \tag{2}$$

In the inset of Fig. 3, we present an autocorrelation function ($f_1=f_2$) calculated from a measured force curve for the interval $20<x'<30$ μm in displacement. The autocorrelation function exhibits one prominent peak of unity height at zero shift Δ. The full width at half maximum (FWHM) of the peak is a measure of the characteristic size in x_0 of the structures in the force curve. As shown in Fig. 3, this FWHM decreases with the translation velocity and shows a tendency of saturation at low velocities. The FWHM of the autocorrelation peak of the calculated force curve is shown as a dotted line. The decrease of the FWHM with the displacement velocity and the tendency of saturation to a value close to the theoretical result (corresponding to zero velocity) suggest that the experimental conditions correspond to a close to equilibrium situation. This contrasts to the situation encountered in AFM measurements of bond breaking where the measured forces are found to increase sizably with the displacement velocity [14]. This point is further discussed in Sec. V.

When the correlation function of two different force versus displacement curves is calculated with Eq. (1), the peak

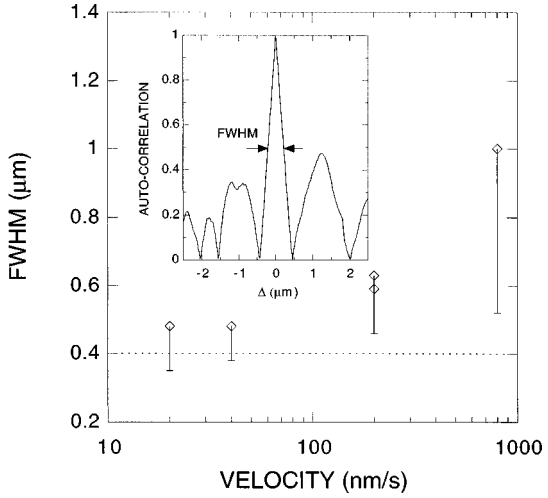

FIG. 3. Full width at half maximum (FWHM) of the autocorrelation function $g(\Delta)$ of the force versus displacement curves as a function of displacement velocity. The function $g(\Delta)$, defined by Eq. (1), is calculated over the interval of displacement $(a,b)=(20,30)$ μm. The horizontal dotted line indicates the FWHM of the correlation function obtained for the theoretical force curve of Fig. 2. The inset shows the autocorrelation function for the case of $v=20$ nm/s, corresponding to the 20 nm/s force curve of Fig. 2. The data points indicated by diamonds correspond to FWHM values derived as indicated by the arrows in the inset. The lower limit of the error bars is obtained when the FWHM is taken after subtraction of the average value of the autocorrelation function in the region outside the central peak.

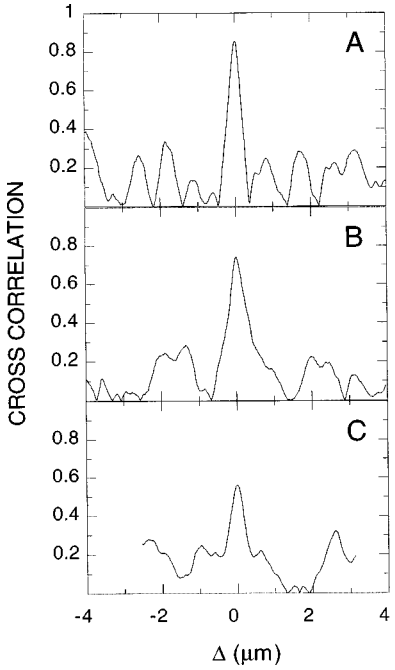

FIG. 4. Cross-correlation functions for (a) two measurements on the same molecule with displacement velocities of 20 nm/s and 40 nm/s, (b) two measurements on two different molecules with 20 nm/s and 40 nm/s, and (c) two measurements on the same molecule with 40 nm/s and 200 nm/s.

height is below one and measures the agreement between f_1 and f_2. As exemplified in Fig. 4, we find peak heights in excess of 0.7 at the lowest displacement velocities, between curves measured on the same or different molecules. The peak values decrease and the FWHM increase with increasing velocity of displacement. Highest resolution and reproducibility is obtained at the smallest velocity of 20 nm/s.

Let us briefly consider the remaining uncertainties in the measurements. The data are collected at room temperature. The corresponding variation in the liquid buffer temperature is below $\pm 5\,^{\circ}$C, which is too small to induce sizable effects. Since the sample is not covered, evaporation can occur during a measurement leading to a gradual rise in the salt content. We add H_2O to the sample between individual measurements but a variation in the salt content of about 20–40 % remains possible. However, for a variation of this size we observe no noticeable changes in the force curves. There is a lateral drift of the sample with respect to the force lever of typically 1 μm over 10 min. We systematically determine the corresponding error by a comparison of the lever positions just before and after the measurement and correct the force curve assuming a constant drift velocity. The experimental results presented in this paper are obtained with a single force lever, which avoids relative errors between different recordings. Only small uncertainties may arise from weak torsion of the lever which can depend on the exact position of the bead on the lever and couple to the measured deflection. At the lowest displacement velocities the reproducibility of the experimental results appears to be limited by mechanical perturbations.

III. THEORETICAL DESCRIPTION

We have developed a theoretical description for the unzippering of DS-DNA by a mechanical constraint. It is based on the interplay of the following four energies within the frame of equilibrium statistical mechanics.

The first energy, called $E_{\mathrm{DNA}}(j)$, describes the work necessary to separate the two single strands of the DNA double helix from the base pair of index 1 to the base pair of index j. Specifically, it includes the contributions of the unpairing, the unstacking, and the rearrangement of the bases. The two elementary pairings in DNA are the G-C and A-T base pairs of Watson and Crick. As a G-C pair is formed through three hydrogen bonds while an A-T one involves only two hydrogen bonds, $E_{\mathrm{DNA}}(j)$ acquires a dependence on the genomic sequence of the DNA under study. To date there is no theory available to quantitatively describe the binding of the DNA base pairs in an aqueous medium. Comparison of melting experiments on short DS-DNA stretches to thermodynamical models including interactions between up to second neighbor base pairs have allowed an estimation of the binding energies between the DNA bases [20,21]. However, a direct application of these energies to our experimental configuration is not justified because melting is driven by fluctuations and therefore strongly depends on the conformations of the free single stranded ends. In our experiment the single strands are under tension. We therefore expect that the only significant entropic energy contribution arises from the rearrangement of the bases after rupture. For the energy E_{pair} corresponding to opening the base pair of index ν, we simply write $E_{\mathrm{pair}}(\nu)=E_{\mathrm{G\text{-}C}}$ if the index ν corresponds to a G-C pair and $E_{\mathrm{pair}}(\nu)=E_{\mathrm{A\text{-}T}}$ if ν corresponds to an A-T pair. $E_{\mathrm{G\text{-}C}}$ and $E_{\mathrm{A\text{-}T}}$ are treated as fitting parameters as described further

below. The potential energy E_{DNA} is then given by

$$E_{\mathrm{DNA}}(j)=\sum_{\nu=1}^{j} E_{\mathrm{pair}}(\nu). \tag{3}$$

Notice that in this model, different base sequences may have the same potential energy $E_{\mathrm{DNA}}(j)$ because interactions between neighboring base pairs are neglected. This means, in particular, that an A-T pair is considered to be equivalent to a T-A one and the same holds for the G-C and C-G pairs.

The second energy, called E_{ext}, is the elastic energy stored in the extended single strands. Force versus extension curves of SS-DNA have been measured by Smith, Cui, and Bustamante [8]. Their data are described by the expression

$$\delta(F)=j_{\max}z(F)=L_{\mathrm{SS}}\left[\coth\left(\frac{Fb}{kT}\right)-\frac{kT}{Fb}\right]\left(1+\frac{F}{S}\right). \tag{4}$$

It relates the total polymer length δ (or the length z per base) to the applied force F in the frame of a freely jointed chain (FJC) model, containing an entropic (coth term) and a stretching (F/S term) contribution. Equation (4) contains three parameters: the contour length L_{SS} of a DNA single strand with $j_{\max}$ bases, the Kuhn length b (which in the FJC model is equal to half the persistence length), and the stretch modulus S. The elastic energy $E_{\mathrm{ext}}(j,\delta)$ corresponding to a single strand of j bases, extended by the force F to a length δ, is obtained from Eq. (4) by numerical inversion and analytical partial integration:

$$E_{\mathrm{ext}}(j,\delta)=F(\delta)\delta-j\int_0^{F(\delta)}dF'z(F'). \tag{5}$$

The extension of the DS-linker arm can be neglected under the present experimental conditions. Regarding the configuration represented schematically in Fig. 1, we see that the system attached to the opening fork corresponds to a serial arrangement of four springs: the DS-DNA linker arm, the left SS-DNA, the right SS-DNA, and the force lever. The total stiffness k_{tot} of this arrangement is given by the harmonic average $k_{\mathrm{tot}}^{-1}=\Sigma k_i^{-1}$ of the stiffness values k_i of the individual springs. The DS-linker arm is much stiffer than the microneedle and, with the exception of the first part of the opening where the single strands are still short, it is also stiff compared to the single stranded parts. This is seen by taking the local stiffness of DS-DNA at the opening force from the literature [7,9,10]. For a force variation of about 1 pN in amplitude around a mean value of 13 pN corresponding to our opening experiment, we thus obtain a variation in the extension of the DS-linker arm of below 0.1 μm. The corresponding change in the lever deflection is 1.2 μm and the corresponding fluctuation in the total length of the two single strands is 1.9 μm for the nearly fully opened case (total single strand length of about 45 μm). The total stiffness, which controls the effect of elasticity on the opening fork, is therefore only weakly influenced by the DS-linker arm. As an experimental confirmation of this fact, we observe no significant difference between measurements performed with linker arms of different length (one λ-DNA molecule compared to two λ DNA in series).

The third energy, called E_{lev}, is the elastic energy of the lever:

$$E_{\mathrm{lev}}=\frac{1}{2}k_{\mathrm{lev}}x^2=\frac{1}{2}k_{\mathrm{lev}}(x_0-\delta_1-\delta_2)^2. \tag{6}$$

The lever deflection x is given by the difference between the sample displacement x_0 and the sum of the length δ_1 of the single strand attached to the microscope slide and the length δ_2 of the single strand attached to the bead.

The fourth energy is the thermal energy kT. Its most important effect arises from the fact that it directly enters the statistical weight in the calculation of the thermal averages in the canonical ensemble [see Eq. (7)]. In addition, the force versus extension relation Eq. (4) exhibits a small temperature dependence. Finally the phenomenological parameters $E_{\mathrm{G\text{-}C}}$ and $E_{\mathrm{A\text{-}T}}$ of Eq. (3) are temperature dependent through their entropic part mentioned above. In this article we do not consider effects of temperature variations and assume a temperature of 300 K, i.e., $kT=25$ meV.

The thermal average of an obvservable A is calculated by the expression

$$\langle A\rangle=\frac{\sum_{j,\delta_1,\delta_2}A(j,\delta_1,\delta_2)e^{-E_{\mathrm{tot}}(j,\delta_1,\delta_2)/kT}}{\sum_{j,\delta_1,\delta_2}e^{-E_{\mathrm{tot}}(j,\delta_1,\delta_2)/kT}}, \tag{7}$$

with the total energy given by

$$E_{\mathrm{tot}}=E_{\mathrm{DNA}}(j)+E_{\mathrm{ext}}(j,\delta_1)+E_{\mathrm{ext}}(j,\delta_2)+E_{\mathrm{lev}}(\delta_1+\delta_2). \tag{8}$$

At given x_0 and j, Eq. (8) exhibits a minimum at the position

$$\delta_1=\delta_2=\delta_0(j,x_0)=jz(F_0). \tag{9}$$

The force value F_0 is given by the implicit expression

$$0=F_0+k_{\mathrm{lev}}[2jz(F_0)-x_0], \tag{10}$$

which is easily solved numerically. A quadratic development of Eq. (8) with respect to δ_1 and δ_2 allows us to analytically perform the integrations over δ_1 and δ_2 by extending the integration interval to $\mp\infty$ in Eq. (7). The discrete summation over j is done numerically.

Any dependence of the total energy on a velocity coordinate has been neglected. In particular, no viscous friction of the lever is included in the model. We have estimated the corresponding forces and found that they are negligible for the small displacement velocities used in the measurements. The rotation of the double helical part of the DNA to be opened and couplings between torsion and linear elasticity are also not considered. As explained above, the elasticity of the molecular construction mainly arises from the single stranded parts. A single strand can, however, easily rotate around the single bonds connecting the sugar and phosphate groups of the covalent DNA backbone. Therefore we do not expect that a significant torsion develops. The central as-

sumption of thermal equilibrium will be discussed further below, in the context of Fig. 7 and in Sec. V.

Our theoretical description contains five parameters, the contour length L_{SS}, Kuhn length b, and stretch modulus S of the SS-DNA [Eq. (4)] and the binding energies $E_{G\text{-}C}$ and $E_{A\text{-}T}$ of the base pairs. The parameters are not really independent: the set $L_{SS}=30$ μm, $b=1.5$ nm, $S=800$ pN, $E_{G\text{-}C}=2.9kT$, $E_{A\text{-}T}=1.3kT$ (set A) describes our data equally well as the set $L_{SS}=27$ μm, $b=2.7$ nm, $S=800$ pN, $E_{G\text{-}C}=3.2kT$, $E_{A\text{-}T}=1.6kT$ (set B). The theoretical results presented in this article are obtained with the parameter set A. The fit values reported by Smith *et al.* for the elasticity of SS-DNA under their experimental conditions are $L_{SS}=27$ μm, $b=1.5$ nm, $S=800$ pN. Our $E_{G\text{-}C}$ and $E_{A\text{-}T}$ values are in the range of the free energy parameters ΔG reported in the literature for the separation of DNA base pairs (see [20,21], and references therein). They are smaller than the corresponding enthalpy parameters ΔH. On the other hand, AFM measurements of rupture forces of different ligand receptor pairs have been found to correlate better with the ΔH than with the ΔG parameter [15]. We attribute the difference to the fact that for bond breaking the entropic contribution corresponding to the rearrangement of the binding partners may occur after rupture and the associated detachment of the lever, while our measurement is sensitive to this contribution as the lever remains connected during the progressive rupture of the base pairs. After breaking the bond there is a sudden separation event with subsequent energy dissipation in the AFM experiments, while in our case the measured force may be seen as an average over the configurations explored by the breathing opening fork.

In Fig. 5 calculated thermal averages of the deflection force F and of the number of opened base pairs j are presented as a function of the sample displacement x_0. Since the amplitude of the force variation during the opening is small with respect to the average opening force, the total single strand length l_0 liberated by opening one base pair is roughly constant. At the average force level of about 13 pN measured during the DNA opening, we have $l_0=2\delta(F)\cong 0.95$ nm from Eq. (4). In this global frame, the average number of opened base pairs $\langle j\rangle$ increases linearly with increasing displacement: $\langle j\rangle = x_0/l_0$. The order of magnitude of the force required to open DNA is related to the energy parameters by $F=[E_{pair}+2E_{ext}(1,l_0/2)]/l_0$. With $E_{pair}=2.1kT$ (average binding energy of a base pair assuming a G-C content of 0.5) and $E_{ext}(1,l_0/2)\cong 0.5kT$ (elastic energy necessary to stretch the single strand segment corresponding to one liberated base, up to the length $l_0/2$) we obtain the measured level of $F\cong 13$ pN.

At a finer scale, as shown in Fig. 5, the thermal average $\langle j\rangle$ does not increase linearly with x_0, but rather as a succession of quasisteps and plateaus. A quasistep in $\langle j\rangle$ corresponds to a decrease in the deflection force $\langle F\rangle = k_{lev}\langle x\rangle$ and a sharp peak in the variances var$j$ and var$F$. On a quasiplateau in $\langle j\rangle$ the force $\langle F\rangle$ increases almost linearly and the variances var$j$ and var$F$ are small. This represents a stick-slip dynamics at the molecular level [18]. It is considered in the following section.

At the top of Fig. 5 we present the normalized correlation (as defined in the caption) between the lengths of the two single strands δ_1 and δ_2. In the regions of high variance in j (slip phases), this correlation function approaches one, indicating almost complete correlation. In this case, the fluctuations in the position of the opening fork dominate and lead to an in-phase fluctuation in the lengths of the two liberated single strands. In regions of low variance in j (stick phases), the normalized correlation is negative. This is readily understood in a simplified picture where we assume an entirely blocked opening fork. There thermal fluctuations are important, for which, avoiding a sizable change in the lever deflection, one of the two strands increases in length and the other one decreases accordingly. This gives rise to an anticorrelation. The deviations of the correlation function from zero show that it is important to consider the thermal fluctuations in δ_1 and δ_2 independently in the theoretical description.

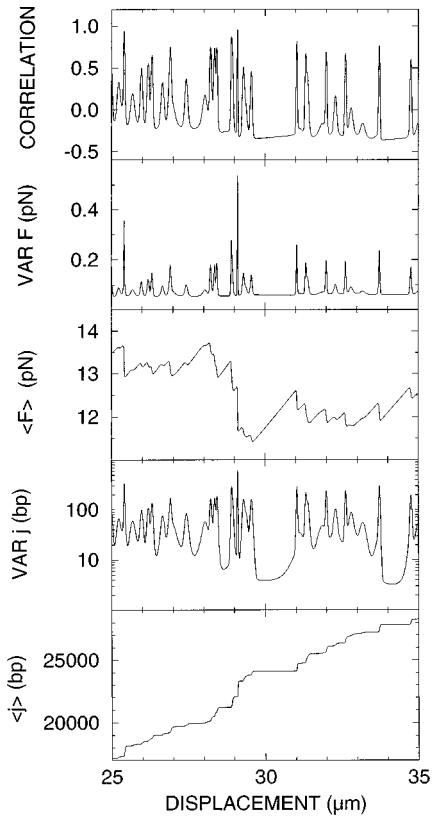

FIG. 5. Theoretical results on the average number of opened base pairs $\langle j\rangle$, the variance of the number of opened base pairs var$j$, the deflection force $\langle F\rangle = k_{lev}\langle x\rangle$, the variance of the deflection force var$F$, and the correlation between the length of the two single strands [correlation $=\langle \delta_1\delta_2\rangle/(\langle \delta_1^2\rangle\langle \delta_2^2\rangle)^{1/2}$].

There are two earlier theoretical studies of the force signals expected upon mechanical separation of the two strands of the DNA double helix in configurations similar to our experiment [28,29]. In both cases, the authors assumed only a simple sinusoidal modulation of the binding energy (the energy E_{DNA} in our notation) at the scale of one base pair. They concluded that the force measurement will not allow one to resolve the opening of an individual base pair and did not predict the process of molecular stick slip. In contrast to the earlier work, we consider a complex sequence of base pairs combined with the elasticity of the single strands and the thermal fluctuations. The intermediate scale variations in the G-C content are important; they are at the origin of the molecular stick-slip motion.

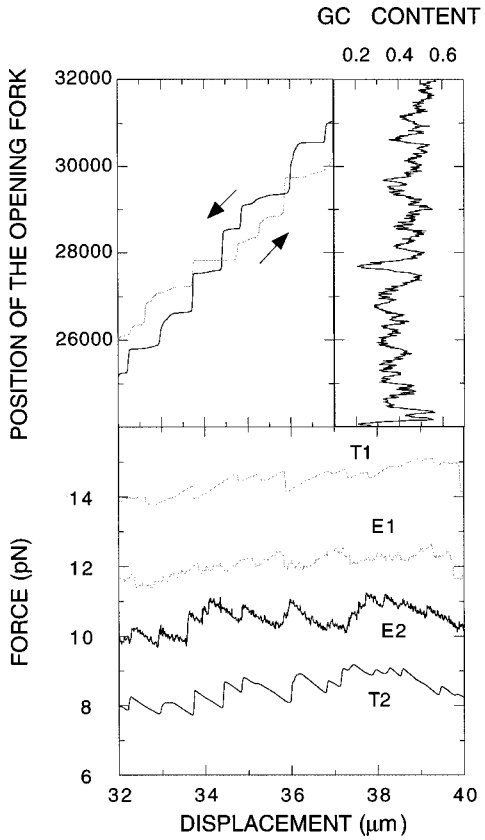

FIG. 6. Bottom: comparison of measured ($E1$,$E2$) and calculated ($T1$,$T2$) force versus displacement curves for opening two different molecular constructions. The black lines ($E2$,$T2$) are for opening of a construction with a sequence of base pairs which is reversed with respect to the usual sense and the horizontal axis is reversed accordingly (opening proceeds from the right to the left part of the figure). The results for opening the same sequence in the usual sense are shown as gray lines ($E1$,$T1$). $E1$ ($E2$) has been measured with a displacement velocity of 40 nm/s (20 nm/s). Top left: calculated thermal averages of the position of the opening fork on the base sequence. Top right: G-C content (sliding average over 100 base pairs) of the corresponding region on the λ-DNA genome.

IV. MOLECULAR STICK SLIP

In this section we first present the experimental manifestations of the molecular stick-slip motion, then show how it is related to the sequence of the base pairs, and finally illustrate the essence of this process in a simple analytical model.

In the bottom of Fig. 6, a measured force curve ($E1$) is shown for a relatively narrow range of sample displacement x_0. It corresponds to opening the double helix from a base index of about 25 000 to about 34 000. On this scale, a sawtoothlike shape of the structures in the measured force signal becomes apparent. Let us assume for the sake of simplicity that the opening fork is fully blocked at a given position on the base sequence. A further increase Δx_0 in the sample displacement then induces a linear rise in the deflection force: $\Delta F = \Delta x_0 k_{\mathrm{eff}}$. The effective stiffness k_{eff} is the harmonic average of the local stiffness k_{SS} of the two single strands in series at the opening force and of the lever stiffness k_{lev}: $k_{\mathrm{eff}}^{-1} = k_{\mathrm{SS}}^{-1} + k_{\mathrm{lev}}^{-1}$. From the measurement of the extension of SS-DNA by Smith *et al.* [8], we obtain $k_{\mathrm{SS}} \cong 1.6$ pN/μm for a strand length corresponding to $x_0 = 36$ μm. With the calibrated k_{lev} of 1.7 pN/μm we thus estimate for the slope of the rising part of the sawtooth a value of $\Delta F/\Delta x_0 \cong 0.8$ pN/μm. This value is close to the slopes observed on the $E1$ curve of Fig. 6.

We have prepared a second molecular construction where the DNA to be opened is incorporated with the base sequence in reversed order. In the presentation of Fig. 1, this corresponds to exchanging the top ends of the center DNA by the bottom ends. This construction allows us to open the same base sequence in opposite sense, i.e., opening proceeds from base index 48 502 down to 1. The curve $E2$ has been measured on such a reversed construction. It is plotted with a reversed horizontal axis. In this presentation, a given value of displacement corresponds on average to the same region on the sequence for the $E1$ and the $E2$ curve. At the scale of Fig. 6, the $E1$ and $E2$ curves are different. The force signal thus depends on the direction of the mechanical opening, while only the gross variations are simply given by an average over the G-C versus A-T content of the DNA. The theoretical curves $T1$ and $T2$ show the same characteristic dependence on the direction of the opening and a reasonable agreement is obtained between the measured and the calculated force signals.

The two curves at the top left show the calculated average position of the opening fork on the base sequence for displacement between 32 and 37 μm (the gray line corresponds to $E1$, $T1$ and the dark line to $E2$, $T2$). They allow us to associate the different structures of the force signals to the average G-C content of the molecule presented on the top right. The other way around, Fig. 6 shows how a variation in the sequence of base pairs induces quasiblocking or rapid advancement of the opening fork, corresponding, respectively, to a gradual rise or a sudden drop in the force versus displacement curve.

We notice that the described molecular stick-slip motion is accounted for by the theoretical description based on the assumption of thermal equilibrium. In this respect it fundamentally differs from macroscopic stick-slip processes, where the slip events proceed far from equilibrium and are accompanied by energy dissipation. The relation between the molecular stick-slip and the macroscopic stick-slip motion is further discussed in Sec. V.

To give a more intuitive picture for the physics of the molecular stick-slip process, we theoretically consider a sequence of E_{pair} values which exhibits an energy step of height Δ at the base pair of index $j = j_{\mathrm{step}}$ and is constant elsewhere.

$$E_{\mathrm{pair}}(j) = E_{\mathrm{av}} \pm \Delta(\Theta(j - j_{\mathrm{step}}) - 1/2). \tag{11}$$

The upper (lower) sign corresponds to an ascending (descending) step in E_{pair}, in the sense of increasing j. Neglecting the elasticity of the single strands, the total energy E_{tot} reads [see Eq. (8)]

$$E_{\mathrm{tot}} = (E_{\mathrm{av}} \mp \Delta/2)j \pm \Delta(j - j_{\mathrm{step}})\Theta(j - j_{\mathrm{step}}) + \frac{1}{2}k_{\mathrm{lev}}(x_0 - 2z_0 j)^2. \tag{12}$$

In analogy to Eq. (4), z_0 presents the length per base of the single strands ($z_0 = L_{\mathrm{SS}}/j_{\mathrm{max}}$, without SS elasticity). Equa-

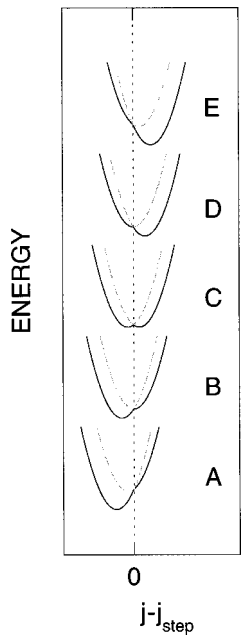

FIG. 7. E_{tot} versus j curves, according to Eq. (12) for a sample displacement x_0 which homogeneously increases from bottom to top. The gray (dark) curves correspond to the case of an ascending (descending) step for opening in the direction of increasing base index j. The curves for different x_0 are shifted vertically for clarity.

tion (12) simply describes segments of quadratic parabola for E_{tot} as a function of j, with minima at the positions

$$j=\frac{x_0}{2z_0}-\frac{E_{\mathrm{pair}}(j)}{4k_{\mathrm{lev}}z_0^2}. \tag{13}$$

In a less compact but more explicit form this equation reads

$$j=\begin{cases}\dfrac{x_0}{2z_0}-\dfrac{E_{\mathrm{av}}\mp\Delta/2}{4k_{\mathrm{lev}}z_0^2} & \text{if } j\leqslant j_{\mathrm{step}}\\[2ex] \dfrac{x_0}{2z_0}-\dfrac{E_{\mathrm{av}}\pm\Delta/2}{4k_{\mathrm{lev}}z_0^2} & \text{if } j>j_{\mathrm{step}}.\end{cases} \tag{14}$$

The curvature at the minimum is always given by $2k_{\mathrm{lev}}z_0^2$, independently of j and the sense of the step. In Fig. 7, we have plotted a series of the E_{tot} versus j curves (x_0 increases linearly from A to E). In the case of an ascending step [gray curves, upper signs in Eqs. (11) and (12)], the minimum reaches the step position from the left (A to B), stays there for a while (B to C, C to D), before it moves further (D to E). In the case of a descending step [black curves, lower signs in Eqs. (11) and (12)], the minimum approaches the step from the left (A to B, B to C), but before it reaches the step a second local minimum appears at the right (C). Further increasing x_0, the latter becomes the total minimum of the curve (C to D, D to E). The described variation of the minimum corresponds to the change in the position of the opening fork in the zero temperature limit. In Fig. 8, top curve, this variation is directly plotted as a function of x_0. The bottom curve gives the corresponding lever deflections $x=x_0-2jz_0$ for the ascending (gray curve) and the descending (black curve) step. We recognize the characteristic features of the stick-slip process, namely, the continuous rise of the deflection when the opening fork approaches an ascending step in the energy landscape and a sudden drop in the deflection when the opening fork passes a descending step.

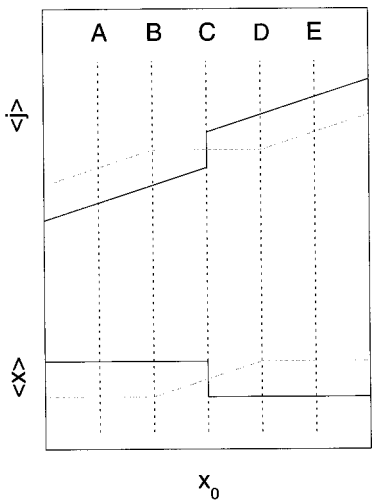

FIG. 8. Top: dependence of the total minimum of the E_{tot} versus j curves on the displacement x_0. Bottom: corresponding lever deflection given by $x=x_0-2z_0j$. As in Fig. 7, the gray lines correspond to an ascending, the dark lines to a descending step.

At nonzero temperature, the opening fork explores the potentials shown in Fig. 7, roughly to an energy of the order of kT above the total minimum. In case C, descending step, these thermal fluctuations are particularly important: the variance in j presents a peak and the average position of the opening fork is given by $\langle j\rangle=j_{\mathrm{step}}$. An important consequence of the thermal motion within the microscopic energy landscape is that the described process of molecular stick slip is deterministic and reversible. The thermal motion is also necessary to assure that the system can always reach the region of the total energy minimum in the parameter space. With increasing displacement velocity in the measurements, this requirement is expected to be increasingly difficult to fulfill within the relevant experimental time scale. We therefore expect a systematic deviation from the equilibrium result, similar to the one observed experimentally (see Fig. 3). In this context, we like to remember that the present theoretical description neglects the dynamics associated to the rotation of the double stranded part occurring as the double helix is pulled open. As the displacement velocity increases, this rotation and also the viscous friction of the lever are expected to become increasingly important.

V. DISCUSSION

Our configuration for the unzippering of DNA by a mechanical constraint applied to the two single strands of the double helix qualitatively differs from the configurations encountered in usual force measurements on the rupture of molecular bonds. In the former case, the molecular system remains attached to the measurement device and an equilibrium deflection is obtained by the thermal breathing of the opening fork which involves opening and reclosing of several base pairings. In the latter case, the mechanical force drives the system from an equilibrium bound state, through a

succession of intermediated states, to a final state where the force lever is disconnected from part of the system, the bond is broken, and the two separated parts have relaxed independently. This process can pass through different sets of intermediate states, which leads to a statistical distribution of the measured rupture force. The average of this distribution typically increases with the velocity used to break the bond [22,23]. This situation is commonly described by molecular dynamics calculations which, at the present stage, however, are limited to time scales which are a few orders of magnitude shorter than the experimental time scale.

Closer to our configuration of DNA unzippering are the recent experiments on stretching of single titin molecules [11–13]. At large extensions, the restoring force of this large muscle protein exhibits a sawtoothlike pattern which has been attributed to the unfolding of individual immunoglobulin domains. Relaxation of the applied force allows one to refold the molecule, similar to the reassociation of the single strands in the case of DNA unzippering. The force required to unfold a single domain is found to increase from about 130 pN to 180 pN when the pulling speed is increased from about 10 nm/s to 500 nm/s [11]. In our experiment, no comparable change in the force signals is observed for a very similar variation in the displacement velocity (Fig. 2). This difference can be associated to the fact that the energy barrier beween a folded and an unfolded domain in the titin molecule is too large to allow for a temperature induced transition. It appears therefore that the measurements on titin are intermediate between the measurements of bond breaking and DNA unzippering: the system remains attached to the force lever and several cycles of unfolding and refolding are possible, but the process of domain unfolding is still far from equilibrium.

Stick slip is commonly observed at the macroscopic level in dry solid friction. This type of behavior has been related to both the elasticity (distributed in the system or localized in the test machine), and the physics of the population of random contact spots between the two solids. Stick slip has the following characteristics. In a first phase, when a constant displacement is imposed via, e.g., an elastic test machine, the two solids have only a little displacement with respect to each other and elastic energy is accumulated. In a second phase, there is a sudden fast sliding with energy dissipation. Afterwards the cycle resumes. Stick slip has been shown to be a very generic phenomenon, occurring between dry solids from the size of a few micrometers with micromechanics up to hundreds of kilometers with earthquakes. Known characteristics of the macroscopic stick-slip process are (i) it is strongly velocity dependent, (ii) it is more or less regular if there is enough averaging (many similar contact spots at any given time), (iii) the interface is usually two dimensional, (iv) the process is dissipative in essence, and (v) the dynamics at very low velocity (below μm/s) has been shown to be related to the irreversible creep of the many localized contact spots (i.e., at a given loading, there is a time-dependent behavior). For the macroscopic stick slip, the reader is referred to [24–27], and references therein.

The molecular situation is completely different, as the molecular stick slip appears to be satisfactorily described in an equilibrium model. The process is (i) one dimensional and related to the sequential exploration of the fixed ''random'' potential landscape created by the complex sequence of the bases along the opening, (ii) it is related to the elastic nature of the system, (iii) the force signal is reversible, and (iv) thermal motion permits an approach to equilibrium.

VI. CONCLUSIONS

Separation of the two strands of a DNA double helix has been achieved by pulling the strands mechanically apart with forces in the range of 10–15 pN. The force measured during the progressive opening of the double helix shows a rapid variation with an amplitude of about 2 pN, which is reproducible to a high degree of detail, both between two measurements performed on the same molecule and between measurements performed on different molecules with the same sequence of base pairs. A theoretical description based on equilibrium statistical physics allows us to relate the force signal to the genomic sequence of the DNA and reproduces the average level and amplitude of the measured force variations. Characteristic sawtoothlike structures appear in the force curves which we associate to a stick-slip motion of the opening fork. In contrast to the classical stick-slip motion, occurring in solid friction, this molecular stick-slip process is reproducible and deterministic. The measured dependence of the force signal on the velocity of the imposed sample displacement indicates that we deal with a close to equilibrium situation. Indeed, a reasonable agreement is obtained between the measurements at low displacement velocity and the calculations based on the assumption of thermal equilibrium.

ACKNOWLEDGMENTS

We thank J. Alsayed, H. Buc, M. Buckle, S. Casaregola, E. Dreyfus, M. Dreyfus, P. Fournier, P. Levinson, P. Lopez, J. L. Sikorav, P. Voisin, and E. Yéramian for fruitful discussions. U. B. thanks the European Union for financial support through the TMR program. The work has been partially supported by the MENESR (ACCSV-5 program). The Laboratoire de Physique de la Matière Condensée (LPMC) is associated with the CNRS (Unité de Recherche Associée 1437) and the Paris VI and VII universities.

[1] H. G. Hansma, J. Vac. Sci. Technol. B **14**, 1390 (1996).
[2] C. Bustamante and D. Keller, Phys. Today **48**(12), 32 (1995).
[3] K. Svoboda and S. M. Block, Annu. Rev. Biophys. Biomol. Struct. **23**, 247 (1994).
[4] R. M. Simmons, J. T. Finer, S. Chu, and J. A. Spudich, Biophys. J. **70**, 1813 (1996).
[5] A. Ashkin, Proc. Natl. Acad. Sci. USA **94**, 4853 (1997).
[6] A. Kishino and T. Yanagida, Nature (London) **334**, 74 (1988).
[7] Ph. Cluzel, A. Lebrun, C. Heller, R. Lavery, J.-L. Viovy, D. Chatenay, and F. Caron, Science **271**, 792 (1996).
[8] S. B. Smith, Y. Cui, and C. Bustamante, Science **271**, 795 (1996).
[9] S. B. Smith, L. Finzi, and C. Bustamante, Science **258**, 1122 (1992).

[10] M. D. Wang, H. Yin, R. Landick, J. Gelles, and S. M. Block, Biophys. J. **72**, 1335 (1997).
[11] M. Rief, M. Gautel, F. Oesterhelt, J. M. Fernandez, and H. E. Gaub, Science **276**, 1109 (1997).
[12] M. S. Z. Kellermayer, S. B. Smith, H. L. Granzier, and C. Bustamante, Science **276**, 1112 (1997).
[13] L. Tskhovrebova, J. Trinick, J. A. Sleep, and R. M. Simmons, Nature (London) **387**, 308 (1997).
[14] E.-L. Florin, V. T. Moy, and H. E. Gaub, Science **264**, 415 (1994).
[15] V. T. Moy, E.-L. Florin, and H. E. Gaub, Science **266**, 257 (1994).
[16] G. U. Lee, D. A. Kidwell, and R. J. Colton, Langmuir **10**, 354 (1994).
[17] A. Noy, D. V. Vezenov, J. F. Kayyem, T. J. Meade, and C. M. Lieber, Chemistry and Biology **4**, 519 (1997).
[18] U. Bockelmann, B. Essevaz-Roulet, and F. Heslot, Phys. Rev. Lett. **79**, 4489 (1997).
[19] B. Essevaz-Roulet, U. Bockelmann, and F. Heslot, Proc. Natl. Acad. Sci. USA **94**, 11770 (1997).
[20] K. J. Breslauer, R. Frank, H. Blöcker, and L. A. Marky, Proc. Natl. Acad. Sci. USA **8**, 3746 (1986).
[21] V. Bloomfield, D. Crothers, and I. Tinoco, *Physical Chemistry of Nucleic Acids* (Harper and Row, New York, 1974).
[22] E. Evans and K. Ritchie, Biophys. J. **72**, 1541 (1997).
[23] H. Grubmüller, B. Heymann, and P. Tavan, Science **271**, 997 (1996).
[24] P. Bowden and D. Tabor, *Friction and Lubrication of Solids* (Clarendon, Oxford, 1950).
[25] Ch. Scholz, *The Mechanics of Earthquakes and Faulting* (Cambridge University Press, Cambridge, England, 1990).
[26] T. Baumberger, F. Heslot, and B. Perrin, Nature (London) **367**, 544 (1994).
[27] K. Heki, S. Miyazaki, and H. Tsuji, Nature (London) **386**, 595 (1997).
[28] J.-L. Viovy, Ch. Heller, F. Caron, Ph. Cluzel, and D. Chatenay, Acad. Sci. Paris. C.R. **317**, 795 (1994).
[29] R. E. Thompson and E. D. Siggia, Europhys. Lett. **31**, 335 (1995).